UNIVERSITI
MALAYSIA
PERLIS

Synthesis and Characterization of Structural, Magnetic and Electrical Properties of Ni–Mn–Zn Ferrites

Hosney Ara Begum[1,a], Nazia Khatun[1,b,*], Suravi Islam[1,c], Nurzaman Ara Ahmed[1,d], Mohammad Sajjad Hossain[1,e], Mohammad Abdul Gafur[2,f] and Ayesha Siddika[2,g]

[1] Industrial Physics Division, BCSIR Laboratories, Dhaka. Bangladesh.
[2] IFRD, BCSIR, Dhaka, Bangladesh.

ABSTRACT

Polycrystalline ferrites ($Ni_XMnZn_{1-X}Fe_2O_4$) were synthesized by a conventional ceramic method and sintered at 1100°C for 4 hours. The structure and surface morphology of the samples were characterized by X-ray diffraction (XRD) and scanning electron microscopy (SEM) analyses. Frequency-dependent permeability (μ'), conductivity (σ), quality factor (Q), dielectric loss ($\tan\delta$), and dielectric constant (ε') of the samples were measured by impedance analyzer. DC resistivity and activation energy were also determined. Activation energy was calculated by Arrhenius-type resistivity plots. Analysis of the microstructure of the prepared sample showed that the average grain size increased with increasing nickel (Ni) content. Based on the XRD patterns, the prepared samples showed a cubic spinel structure and an average crystalline size of 46 nm.

Keywords: Microstructure, Grain size, Curi temperature (T_c), Dielectric Constant (ε') and Conductivity (σ).

1. INTRODUCTION

Since the discovery of ferrites, the design and synthesis of ferrites have been the focus of intense fundamental and applied research as such to improve the physical properties of ferrite. Ferrite materials are widely used in electronic devices such as sensors, memory storing apparatus, electromagnetic gadgets, and actuators. Soft magnetic ferrites such as those based on oxides, are the most important [1]. Scholars have reported on the advantages of nano-crystalline ferrites particularly nano-sized zinc that interacts with other mixed ferrites [2,3].The magnetic and electric properties [4] of these materials have gained increasing research attention[5]. Mn–Zn ferrites are extensively used in electronics due to high saturation magnetization, magnetic permeability, and dielectric resistivity and low core losses [6,7]. Similar to Mn–Zn ferrites, Ni–Zn ferrites play a vital role in the technological field.

The combination of the Mn–Zn and Ni–Zn, namely, Ni–Mn–Zn ferrite, may produce good magnetic properties and can be applied in high frequency regions [8].The dielectric properties of Ni–Mn–Zn ferrites should be further studied considering only few works have been conducted on these materials [9]. These ferrites can be synthesized through co-precipitation, hydrothermal process, solution–gel technique, high-energy ball milling, and conventional ceramic method [10–15]. In the present work, conventional ceramic method was used for

synthesis. The density, porosity, and initial permeability of $Ni_xMnZn_{1-x}Fe_2O_4$ were systematically evaluated to investigate the electric and magnetic properties of Ni–Mn–Zn ferrites and extend their application in high frequency regions.

2. MATERIALS AND METHODS

Polycrystalline $Ni_xMnZn_{1-x}Fe_2O_4$ was prepared through a simple conventional ceramic method. Analytical-grade manganese oxide (MnO_2), nickel oxide (NiO), zinc oxide (ZnO), and ferric oxide (Fe_2O_3) were used as raw materials. Stoichiometric amounts of raw materials were mixed in a soggy medium to facilitate homogeneous mixing. Aluminum balls were used to prevent iron contamination, and ethanol was added to form homogeneous slurry. The samples were pulverized through a planetary ball mill for 8 hours. The weight ratio of the ball to powder was 10:1. The milled samples were calcined in a furnace at 700°C for 3 hours in the presence of air. The dried powder was ball milled for 2 hours. The ground ferrite powder was plasticized with an aqueous solution of 4% polyvinyl alcohol (PVA) as binder. The resulting materials were pressed into pellets and toroidal shape by applying 3±0.5 MPa for 1 minute. The samples were then sintered at 1100°C for 4 hours.

3. RESULTS AND DISCUSSION

$Ni_xMnZn_{1-x}Fe_2O_4$ ferrites were characterized by X-ray diffraction (XRD) and scanning electron microscopy (SEM) analyses. The XRD analysis showed a single phase patterns indicating that the sample is ferrite with a cubic spinel structure. All XRD peak in Figure 1 is at (220), (311), (222), (400), (422), (511), and (400) planes. Generally, the intensity of the XRD peak changes when the structure is altered. Such changes also depend on the atomic position, type and quantity in the cell. In addition, grain size, grain surface relaxation and temperature also influence the variations in the peak intensity.
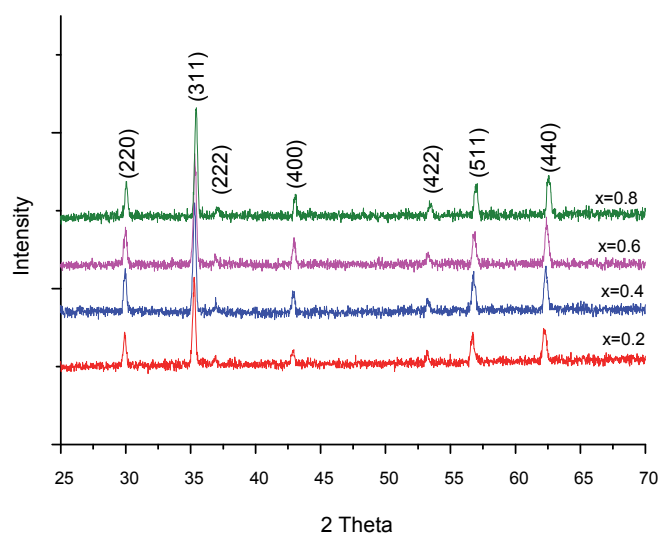

Figure 1. XRD pattern of $Ni_xMnZn_{1-x}Fe_2O_4$ (where x= 0.2, 0.4, 0.6, 0.8)

By using the Debye Scherrer equation in Eq. (1), the average crystallite size can be determined from the (311) diffraction peak, which exhibited the highest intensity.

$$D_{xrd} = \frac{0.9 \times \lambda}{\beta cos\theta} \tag{1}$$

where λ is the wavelength of X-ray (1.5406Å), β is the full width at half maximum (in radians), and θ is the Bragg's angle. The lattice parameter of the cubic samples was calculated from d-spacing corresponding to the strongest peak (311) according to the following relation:

$$a = d_{hkl}\sqrt{(h^2 + k^2 + l^2)} \tag{2}$$

where h, k, and l represent the Miller indices of the crystal planes.

Table 1 shows the lattice constant, X-ray density, bulk density, and porosity of the samples. The lattice parameters of all samples were plotted against Ni content as shown in Figure 2. Results indicate that the lattice constant decreased with increasing Ni content. The lattice parameter was then used to calculate X-ray density.
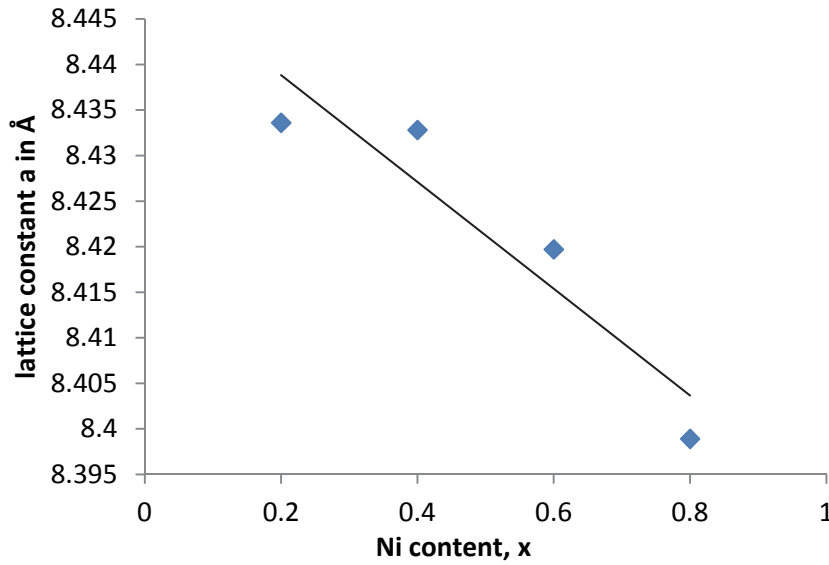

Figure 2. Variation in the lattice constant with Ni content

The relation between X-ray density, ρ_x and lattice constant, a is as follows:

$$\rho_x = \frac{8M}{Na^3}\left(\frac{gm}{cm^3}\right) \tag{3}$$

where N is the Avogadro's number (6.023×10^{23} m^{-1}), and M is the molecular weight. The actual density of the ferrite samples was determined using the Archimedes' principle. The porosity (%P) of the samples was then calculated using the following equation:

$$P = (1 - \rho_a/\rho_x) \times 100 \tag{4}$$

where ρ_a is the actual density of the sample determined using the formula in Eq. (5):

$$\rho_a = \frac{m}{v} \tag{5}$$

where m is the sample weight, and v is the sample volume.

Table 1 Lattice constant, X-ray density, bulk density, and porosity of the samples

Ni content	lattice constant a in Å	X-ray density, gm/cc	Bulk density, gm/cc	Porosity, P (%)
X=0.2	8.4336	6.1928	4.9554	19.9798
X=0.4	8.4328	6.1649	4.9554	18.0408
X=0.6	8.4197	6.1639	4.9699	19.3708
X=0.8	8.3989	6.1798	4.7291	23.4748

The microstructure of $Ni_xMnZn_{1-x}Fe_2O_4$ ferrites was examined through SEM analysis and the images was provided in Figure 3. The microstructure of the synthesized sample shows normal grain growth, uniform and homogeneous distribution of Ni-Mn-Zn ferrites.
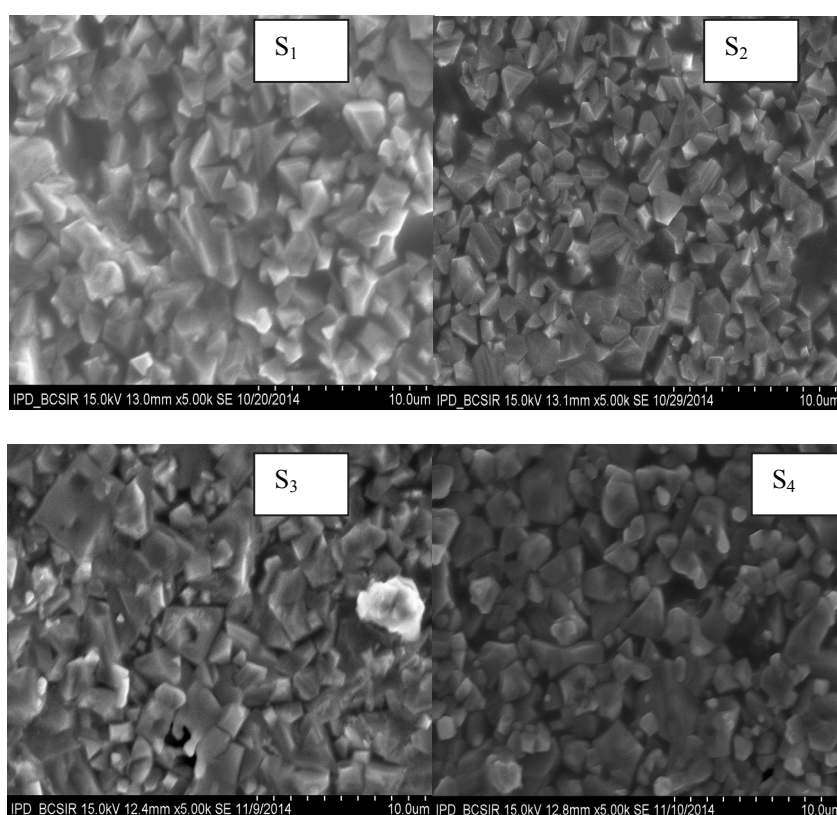

Figure 3. SEM images of $Ni_xMnZn_{1-x}Fe_2O_4$, where Sample 1(S_1) X= 0.2; Sample 2 (S_2) X= 0.4; Sample 3 (S_3) X= 0.6; and Sample 4 (S_4) X= 0.8

The average grain size was calculated from the microstructure of the surface in the SEM image. The results are as follows: S_1 = 0. 656 μm, S_2 = 1.083 μm, S_3 = 1.179 μm, and S_4 = 1.0180 μm. Grain diameter was determined eight or ten times at random, and the average value was obtained. The change in the grain size could be due to the increase in the Ni content, that is, the grain size increased with increasing Ni content. Moreover, the ionic radii of Ni increased when the particle size was increased. The grain size increased when Ni content was set as X=0.6 and decreased thereafter. Table 2 and Figure 4 show the changes in grain size with increasing Ni content.

Table 2 Grain size variation in $Ni_xMnZn_{1-x}Fe_2O_4$ samples

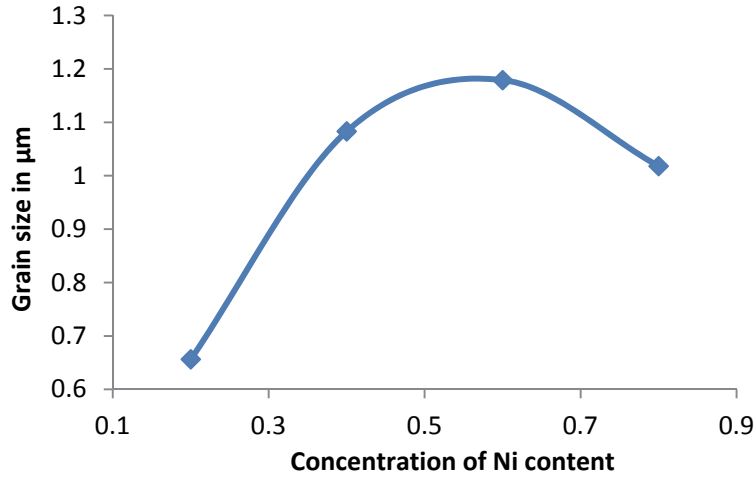| Composition	Grain size (μm)
$Ni_{0.2}MnZn_{0.8}Fe_2O_4$	0.656375
$Ni_{0.4}MnZn_{0.6}Fe_2O_4$	1.083
$Ni_{0.6}MnZn_{0.4}Fe_2O_4$	1.179
$Ni_{0.8}MnZn_{0.2}Fe_2O_4$	1.0180

Figure 4. Concentration of Ni versus grain size

Based on the Arrhenius' relation, activation energy was calculated using the formula:

$$\rho = \rho_0 \exp^{(E_a/kT)} \tag{6}$$

where E_a is the activation energy, k is the Boltzmann constant, and ρ is the resistivity at absolute temperature, T. The results are shown in Table 3.

Table 3 Variations in the Curie temperature and activation energy of $Ni_xMnZn_{1-x}Fe_2O_4$ samples

No. of sample	Composition	Resistivity Ω-cm in room temperature	Curi temperature (K)	Activation Energy E_a in eV
1	$Ni_{0.2}MnZn_{0.8}Fe_2O_4$	8.456×10^6	383	0.5289
2	$Ni_{0.4}MnZn_{0.6}Fe_2O_4$	9.163×10^6	413	0.4128
3	$Ni_{0.6}MnZn_{0.4}Fe_2O_4$	1.5295×10^7	498	0.3986
4	$Ni_{0.8}MnZn_{0.2}Fe_2O_4$	1.5691×10^7	458	0.3954

Figure 5 shows the plot of the Curie temperature (T_c) of the sample versus 1000/T. The Curie temperature (T_c) is an essential property of ferromagnetic materials. The $\ln\rho$ versus 1000/T curves of all the samples were of the same characteristics up to a definite temperature. As shown in Table 3 and figure 6(a), the value of T_c increased from sample S_1 (x=0. 2) to S_3 (x=0. 6) but decreased in S_4 (x=0.8). Figure 6(b) shows the activation energy slightly decreased with Ni content, and this result is similar to the report by Sattar et al. [16]. Moreover, the resistivity and

T_c increased with Ni content. The increase in the T_c could be attributed to the decrease in the A–B interaction. As the Ni content increases, the relative number of Fe^{2+} ions on the A site increases, thereby reducing the A–B interaction [17].
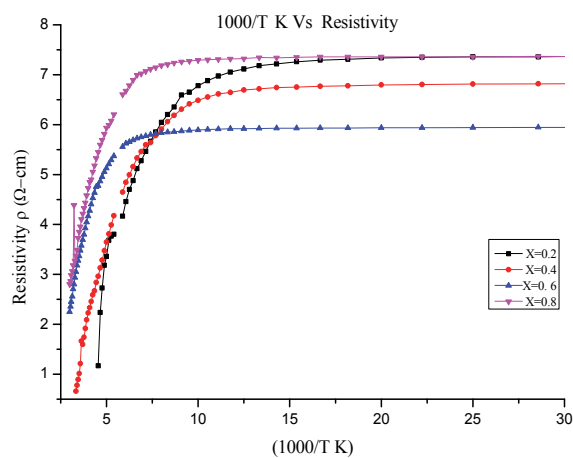

Figure 5. 1000/T versus resistivity of $Ni_xMnZn_{1-x}Fe_2O_4$.
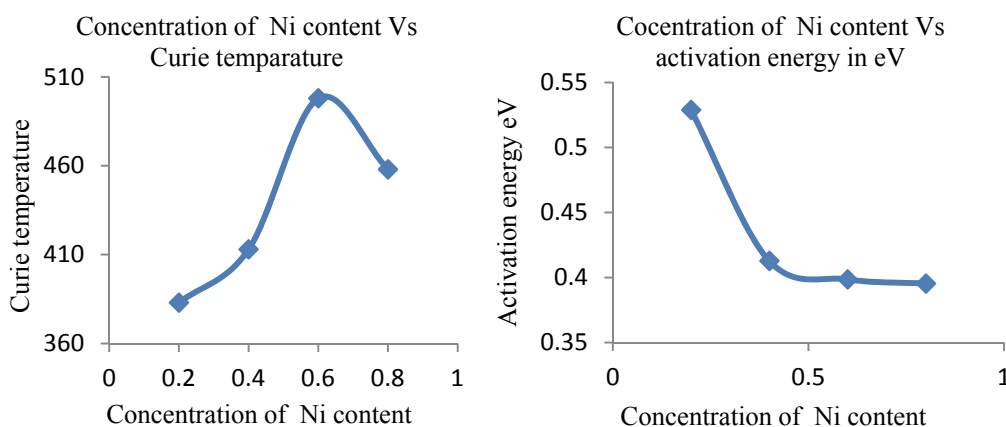

Figure 6. (a) Concentration versus Curie temperature and (b) Concentration versus activation energy

The frequency dependence of dielectric constant ($\acute{\varepsilon}$) for all the samples was studied at room temperature. Figure 7 (a) shows the variation in dielectric constant with frequency. The value of $\acute{\varepsilon}$ decreased continuously with increasing frequency. The frequency dependence of the samples (Ni–Mn–Zn ferrites) showed a normal dielectric behavior, similar to that described by Radha and Ravinder [18]. This reduction occurs because beyond a certain frequency of the externally applied electric field, the electronic exchange between $Fe^{2+} \leftrightarrow Fe^{+3}$ ions cannot follow the alternating field. This behavior is in good agreement with the result of our previous work [19].

According to Refs. [20] and [21], the conduction mechanism of ferrites is strongly correlated with their dielectric behavior. The variation in dielectric loss with frequency is shown in Figure 7 (b). The dielectric loss decreased when the frequency of the applied AC electric field is lower than the hopping frequency of electrons between Fe^{+2} and Fe^{+3} ions at neighboring octahedral sites where the electrons follow the field leading to maximum loss. At high frequencies of the applied electric field, the hopping frequency of the electron exchange cannot follow the applied field beyond certain critical frequency, and the loss is at the minimum. The maximum $\tan\delta$ of

$Ni_xMnZn_{1-x}Fe_2O_4$ was observed at 75 KHz, and the minimum dielectric loss tangent value was detected at 10 MHz frequency. The tanδ decreased gradually with increasing frequency.

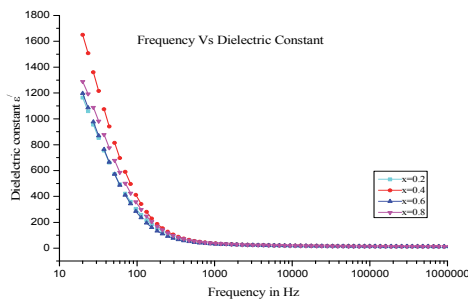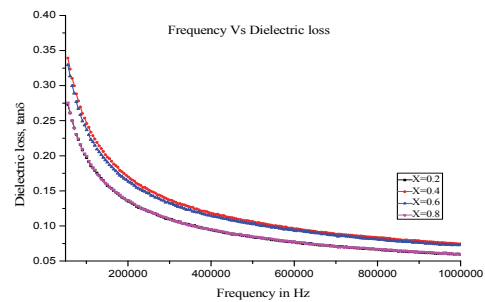**Figure 7 (a)**. Frequency versus dielectric constant   **Figure 7 (b)**: Frequency versus dielectric loss

The variations in AC resistivity and conductivity are shown in Figure 8 (a) and 8 (b) respectively. The AC resistivity and conductivity of Ni–Mn-Zn ferrites were collected frequency range of 1 MHz to 10 MHz at room temperature by using an impedance analyzer. The AC resistivity decreased with increasing frequency. By contrast, the AC conductivity (σ) increased with increasing frequency for all the samples. Thus, the resistivity and conductivity showed opposite characteristics in response to the frequency. Koops theory and Maxwell–Wanger theory [22–24] explained that the AC conductivity increases with increasing frequency, and this trend is in agreement with experimental results in this study. The frequency dependence of resistivity can be explained by the Verwey's hopping mechanism [25]. At low frequencies, the grain boundaries are active and the hopping activities of ferrous and ferric (Fe^{2+} & Fe^{+3}) ions are low. As the frequency of the applied field increases, the conductive grains become more active, thereby promoting the hopping mechanism between Fe^{2+} and Fe^{+3} ions and increasing the hopping conduction. The conductivity gradually increased with frequency.
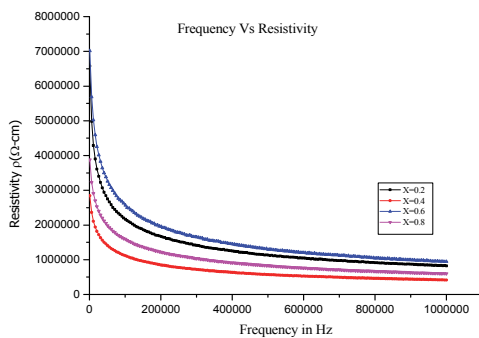

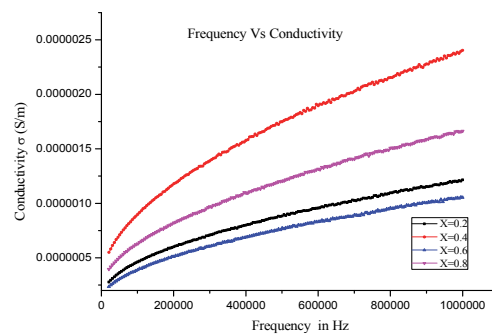**Figure 8 (a)**. Frequency versus resistivity   **Figure 8 (b).** Frequency versus conductivity

Figure 9 shows the plot of initial permeability as a function of frequency for the samples sintered at 1100°C. The value of μ_i increased with increasing Ni content because of increased grain size and enhanced magnetization [26]. The initial permeability of the sample was influenced by the frequency. Hence, high initial permeability can be obtained by increasing the Ni concentration, but the frequency stability decreases. Moreover, the permeability decreased rapidly in low frequency regions and becomes almost constant. The permeability of ferrites is associated with two types of mechanisms, namely, spin rotation magnetization inside the domains and domain wall motion [27–28]. Figure 10 shows the plot of frequency versus Q-

factor for Ni–Mn–Zn ferrites. The Q-factor increased gradually with increasing frequency. Ferrites exhibit high Q-factor and DC resistivity of the order of 10^6 Ω-cm and thus are very useful for transformer core applications up to few MHz frequencies.
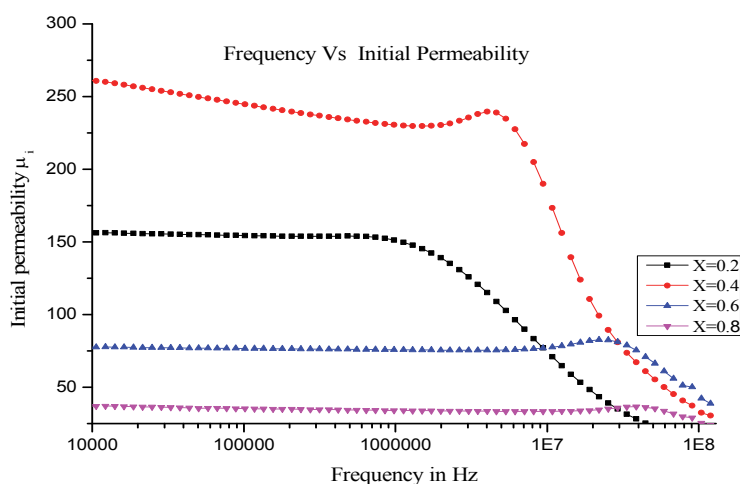

Figure 9. Frequency versus initial permeability

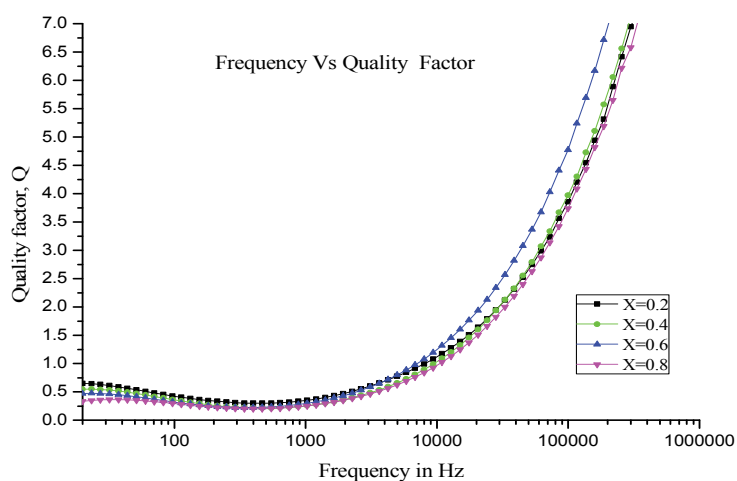**Figure 10.** Frequency versus quality factor

4. CONCLUSIONS

In this study, $Ni_XMnZn_{1-X}Fe_2O_4$ ferrites which play an important role in enhancing magnetic, electrical, and dielectric properties was successfully synthesized. Both the bulk and X-ray densities of the samples decreased with increasing Ni content. The XRD pattern confirmed the single-phase cubic spinel structure. Magnetic properties, such as initial permeability, were also assessed as a function of frequency. The real part of permeability decreased gradually with increasing Ni content. The decrease in the dielectric constant with increasing frequency could be due to the electronic exchange between Fe^{2+} and Fe^{3+} ions in octahedral sites, and this exchange does not follow the frequency of the applied AC field. When increasing Ni content, the Curie temperature and DC resistivity increased but the activation energy decreased. These

experimental results provide a basis for the promising high-frequency applications of ferrite materials.

ACKNOWLEDGEMENT

REFERENCES

[1]   C. Kittel, "Introduction to Solid State Physics," 7th ed., John Wiley and Sons Inc., 1996.
[2]   J. Ding, W. M Miao, P. G McCormick, R. Street, "Mechanochemical synthesis of ultrafine Fe powder", Appl. Phys. Lett. **67** (1995) 3804.
[3]   J.Campbell, W. A. Kaczmarck, G. Wang ,"Mechanochemical transformation of haematite to magnetite" ,Nanostruct. Mater. **6** (1995) 735.
[4]   J. Wang, C. Zeng, Z. Peng, Q. Chen," Synthesis and magnetic properties of $Zn_{1-x}Mn_xFe_2O_4$ nanoparticles", Physica B **349** (2004) 124.
[5]   A.H. Morrish, P.E. Clark, "High-field Mössbauer study of manganese-zinc ferrites", Phys. Rev. B **11** (1975) 278.
[6]   U. Ghazanfar, S. A. Siddiqi, G. Abbas, "Structural analysis of the Mn–Zn ferrites using XRD technique", Mater. Sci. Eng. B **118** (2005) 84.
[7]   G. Ott, J. Wrba, R. Lucke, "Recent developments of Mn–Zn ferrites for high permeability Applications", J. Magn. Magn. Mater. 254-255 (2003) 535.
[8]   A. K. Sing, T.C. Goel, R.G. Mendiratta, "Dielectric properties of Mn-substituted Ni-Zn Ferrites", J. Appl. Phys., **91** (2002) 6626.
[9]   G. F. Dionne, R.G. west, "Magnetic and Dielectric Properties of the Spinel Ferrite System $Nio_{.65}Zno_{.35}Fe_{2-x}Mn_xO_4$", J. Appl. Phys. **61** (1987) 3868.
[10] R. Arulmurugan, B. Jeyadevan, G. Vaidyanath, S. Sendhilnathan,"Effect of zinc substitution on Co–Zn and Mn–Zn ferrite nanoparticles prepared by co-precipitation", J. Magn. Magn. Mater. **288** (2005) 470.
[11] A. Chatterjee, D. Das, S. K. Pradhan, D. Chakravorty, "Synthesis of nanocrystalline nickel-zinc ferrite by the sol-gel method", J. Magn Magn. Mater. **127** (1993) 214.
[12] X. L. Jiao, D. R. Chen, Y. Hu, "Hydrothermal synthesis of nanocrystalline $M_xZn_{1-x}Fe_2O_4$ (M=Ni, Mn, Co; x=0.40–0.60) powders", Mater. Res. Bull. **37** (2002) 1583.
[13] D.J. Fatemi, V.G. Harris, V.M. Browning, J.P. Kirkland, "Processing and cation redistribution of MnZn ferrites via high-energy ball milling", J. Appl. Phys. **83** (1998) 6867.
[14] J. Ding, P. G. McCormick, R. Street, "Formation of spinel Mn-ferrite during mechanical Alloying", J. Magn. Magn. Mater. **171**(1997) 309.
[15] V. Sepelak, A. Buchal, K. Tkácová, K. D. Becker, "Nanocrystalline Structure of the Metastable Ball-Milled Inverse Spinel-Ferrites", Mater. Sci. Forum **278** (1998) 862.
[16] A. A. Sattar, H. M. El-Sayed, W. R. Agami, A. A. Ghani, "Magnetic Properties and Electrical Resistivity of Zr^{4+} Substituted Li-Zn Ferrite", American Journal of Applied Sciences, **4**, Issue 2, Pages 89-93, 2007.
[17] R. C. Kambale, P. A . Shaikh, C. H. Bhosale, K. Y. Rajpure and Y. D. Kolekar, "Dielectric properties and complex impedance spectroscopy studies of mixed Ni-Co ferrites", Smart Mater. Struct, **18**(2009) 0850149(6pp)
[18] D. Ravinder, K. Vijay Kumer, "Dielectric behaviour of erbium substituted Mn-Zn ferrites". Bulletin of Material Science, **24**, Issue 5, October 2001, pp.505-509.

[19] M. Shahjahan, N. A. Ahmed, S. N. Rhaman, S. Islam, N. Khatun, M. S. Hossain "Structural and Electrical Characterization of Li-Zn Ferrites". International Journal of Innovative Technology and Exploring Engineering exploring engineering (Ijitee), **3**, Issue-8, January 2014.

[20] K. Iwauchi "Dielectric properties of fine particles of Fe_3O_4 and some ferrites" Japanese Journal of Applied Physics, **10**, 1971, pp.1520-1528.

[21] *N. Rezlescu*, *E. Rezlescu*, "Dielectric Properties of Copper Containing Ferrites," *Physica Status Solidi (A)*, **23**, No. 2, *1974*, pp. *575*-582.

[22] Maxwell, James Clerk, "A Treatise on Electricity and Magnetism" Oxford: Clarendon Press, Publication date 1873 .

[23] K. W. Wagner, "Zur Theorie der unvollkommenen Dielektrika"Ann Physics Leipzig, **40**, (1913) 817.

[24] C. G. Koop's," On the dispersion of resistivity and dielectric constant of some semiconductors at audio frequencies", Phys. Rev. **83** (1951) 121-126.

[25] Rekha Rania, J. K. Juneja, K. K. Raina, Chandra Prakash, "Studies of the dielectric and ferroelectric properties of PZT: NZF magnetoelectric composites Ceramic Processing" Research. **13**, (2012)76.

[26] N. Rezlescu, E, Rezlescu, P. D. Popa, M. L. Craus, L. Rezlescu, "Copper ions influence on the physical properties of a magnesium-zinc ferrite", Journal of Magnetism and Magnetic Materials, **182**, Issuse 1-2 (1998) pp 199-206.

[27] M. M. Rahman , P. K. Halder , F. Ahmed , T. Hossain, M. Rahaman,"Effect of Ca- substitution on the Magnetic and Dielectric Properties of Mn-Zn Ferrites" J. Sci. Res. **4** (2), (2012) 297-306 .

[28] Md. Mamun-Or-Rashid, Humayun Kabir, Mashudur Rahaman, Md. Abdul Gafur, A.T.M.K. Jamil, Syed Jamal Ahmed , Abdulla Al Noman, Farid Ahmed, "Investigation of the Structural, Dielectric and Electrical properties of Zn-substituted Li-Ni ferrite" IOSR Journal of Applied Physics (IOSR-JAP) E-ISSN: 2278-4861. **7**, Issue 5 Ver. I (Sep. - Oct. 2015), PP 76-83

[29] Zhilun Gui, Ji. Zhou, Longtu Li, Xiaohui Wang, Zhilun Gui, "Effect of Copper On the Electromagnetic Properties of Mg-Zn-Cu Ferrites Prepared by Sol-gel Auto Combustion Method." Materials Science and Engineering: B **86**, Issue 1 (2001) pp 64- 69 .